

ADIABATIC DAMPING DURING ACCELERATION IN THE INDUCTION SYNCHROTRON*

Tanuja Dixit[#], The Graduate University for Advanced Studies, Hayama, Miura, Kanagawa
240-0193, Japan

Yoshito Shimosaki, Ken Takayama, Accelerator Laboratory, High Energy Accelerator Research
Organization (KEK), 1-1 Oho, Tsukuba, Ibaraki, 305-0801, Japan

Abstract

It was observed that a bunch-length shrunk with acceleration in the Induction Synchrotron (IS) experiment, where a single proton-bunch injected from the 500 MeV Booster was accelerated to 6 GeV in the KEK-PS. A novel technique capable of quantitatively predicting the adiabatic phenomenon of bunch shortening has been developed, based on a hypothesis that the particle oscillation amplitude varies inversely proportional to the square root of its oscillation frequency. The experimental result and analytical prediction is in good agreement with each other.

INTRODUCTION

The induction acceleration experiment was carried out using the KEK 12 GeV proton synchrotron (12GeV-PS) in a series of experiments to demonstrate a proof of principle of the IS [1]. Details of the experiments have been described in the literatures [2,3,4,5].

A specific property of the functional separation of acceleration and confinement in the IS allows us to control the beam size through the entire period of acceleration. However, the accelerated beam bunch is subjected to adiabatic damping, as seen in the conventional RF synchrotron. It is quite important to know how the bunch size evolves through the entire acceleration in the IS and what factors dominantly determine the bunch size. A theoretical approach to predict the temporal evolution of the bunch size is developed. After the approach is carefully justified by comparing with computer simulations, the theoretical prediction is compared with the experimental results. Last we will discuss how this theoretical approach can provide a useful tool to estimate a temporal evolution of the bunch size associated with adiabatic changes in the external parameters, such as the barrier voltage amplitude and a time-interval between barrier voltages. It is noted that longitudinal space charge effects are not taken into account in the present discussions because longitudinal space charge forces were small compared to confinement voltage provided during the experiment.

EXPERIMENTAL RESULTS

The bunch profile which was monitored by the wall current monitor, was recorded every 33 msec from the injection to the end of acceleration.

*work supported by a Grant-In-Aid for Creative Scientific Research (KAKENHI 15GS0217)

[#]tanuja@www-accps.kek.jp

Experimental results through the entire acceleration period are plotted for typical four shots in Fig. 1, where the bunch size is defined as a width measured at 5% of the peak height. From Fig. 1, we can clearly identify four regions: At the injection (I), the bunch width is 100 nsec but it quickly increases to ~ 400 nsec because of mismatching to the barrier bucket [3]. Tumbling of the bunch in the phase space and the succeeding filamentation are apparent there, leading to a long bunch width. In the remaining minimal field region (II) before acceleration, the bunch size is almost constant. This implies good matching with the barrier bucket shape throughout the region. The initial acceleration region (III) is characterized by serious beam loss [4]. Quick shrinking of the beam size is caused by the beam loss in addition to damping associated with acceleration. The reason of beam loss is not fully understood, although it is speculated that the control of the trigger pulse density is not enough at this transient region. There is no beam loss in the constant acceleration region (IV). A steady state damping is clear. Near the end of acceleration region, the bunch width is almost constant. We will discuss more about this region hereafter.

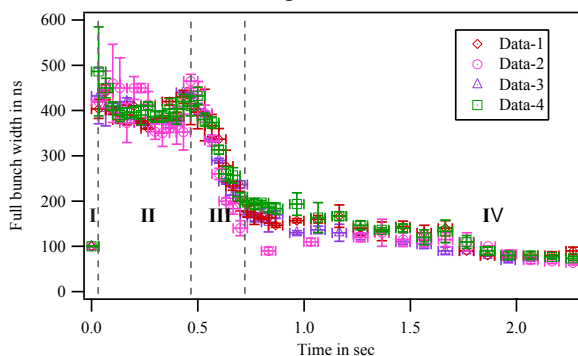


Figure 1: Evolution of the bunch length in time.

THEORY

To develop the theory, we set a hypothesis that the phase oscillation evolves such that the instantaneous oscillation amplitude is inversely proportional to the square root of the phase oscillation frequency. This hypothesis is originated from an analogy of the WKB solution for a harmonic oscillator with slowly varying parameters. Note that the phase motion of a particle trapped in the barrier voltages strongly depends on the oscillation amplitude; in this sense, the motion is a nonlinear motion.

Here, an analytical formula to give the temporal evolution of the oscillation amplitude, which represents an outer bunch-edge, is briefly introduced below [6].

For simplicity, the induction cells for acceleration and confinement are represented by a single device in the present acceleration model. Two dynamical variables of energy E and phase ϕ are used. The former is the total energy of a particle. The latter is defined by $\omega_s t$, where ω_s is the angular revolution frequency of the ideal particle (synchronous particle) and t is time. Note that the synchronous particle is always accelerated with the designed acceleration voltage V_{ac} , which is uniquely determined by the magnetic ramping pattern of accelerator in terms of $\rho C_0 dB/dt$, where ρ is the bending radius, C_0 is the machine circumference, and B is the magnetic flux density. Its dynamical variable has a subscript “s”. These dynamical variables are measured right before entering the above representative acceleration device. Introducing $W = \Delta E/\omega_s$ and $(\Delta E = E - E_s)$, changes in W and ϕ per turn can be given by

$$\begin{cases} \frac{dW}{dt} = \frac{e[V(\phi) - V_{ac}]}{2\pi} \\ \frac{d\phi}{dt} = \frac{\omega_s^2 \eta}{(\beta_s^2 E_s)} W \end{cases}, \quad (1)$$

where e is the unit charge, $V(\phi)$ is the induction voltage seen by a particle, $V(\phi) = V_{bb} + V_{ac}$, η is the slippage factor defined by $1/\gamma_T^2 - 1/\gamma_s^2$ (γ_T is the transition gamma of the accelerator ring) and β and γ are the relativistic beta and gamma, respectively. We assume the barrier voltages V_{bb} with a trapezoidal profile as depicted in Fig. 2a. As the parameters of η , β_s , γ_s , E_s , and ω_s can be regarded as constant for a short time period of the single synchrotron period, the orbit in the phase space is closed; it is nothing but the contour derived from the Hamiltonian, which mimics the barrier bucket shape as depicted in Fig. 2b. The motion in the barrier bucket is qualitatively divided into three regions: (I) focusing in the linear potential, (II) focusing in the parabolic potential, and (III) drift in the null voltage region. It is noted that the motion in region (I) and (II) is subject to adiabatic damping. In addition, it is emphasized that the exact solution throughout the region is known for the above short time period.

To analyze the temporal evolution of this oscillation amplitude associated with acceleration, we start from the canonical Eq. (1). From Eq. (1), a temporal change in the phase of an individual particle is governed by Eq. (2).

$$\frac{d^2\phi}{dt^2} - \frac{(dA/dt)}{A(t)} \cdot \frac{d\phi}{dt} + \frac{eV_{bb}(\phi)A(t)}{2\pi} = 0, \quad (2)$$

where the abbreviation $A(t) = |\eta| \omega_s^2 / \beta_s^2 E_s$ is used for energy below transition energy.

To eliminate the damping term, a new variable $u(t) = \phi(t)/v(t)$ is introduced. When $v(t) = A^{1/2}$, Eq.(2) reduces to

$$\frac{d^2u}{dt^2} + \left[\frac{d^2A/dt^2}{2A(t)} - \frac{3}{4} \frac{(dA/dt)^2}{A^2(t)} \right] u(t) + B(t) = 0, \quad (3)$$

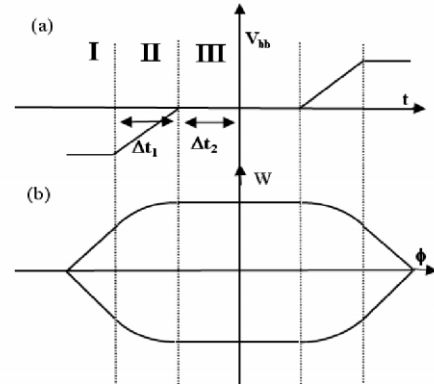


Figure 2: (a) Barrier voltage profile with three distinct regions and peak height of V_0 . (b) Typical trajectory in the phase space.

where $B(t) = eV_{bb}(\phi)A^{1/2}/2\pi$. Since $A(t)$ is a slowly varying function of time, its first-order and second-order time-derivatives are small. So, we arrive at a final form of the phase oscillation equation that must be substantially solved, $d^2u/dt^2 = -B(t)$. The restoring force $B(t)$ can be assumed to be constant during a single synchrotron oscillation period T , which is much shorter than $1/(dA/dt)/A$. In addition, the synchrotron oscillation is symmetric in the phase space, as depicted in Fig. 2b. If we obtain exact solutions in three regions of I, II, and III in Fig. 2a, the synchrotron frequency $\Omega_s = 2\pi/T$ is written in an analytic form [6]. From the hypothesis, the instantaneous amplitude of the phase, $\langle\phi\rangle$, is given by

$$\langle\phi\rangle = C \frac{\sqrt{A}}{\sqrt{\Omega_s}}, \quad (4)$$

where C is a constant coefficient determined from the initial condition. Introducing the instantaneous oscillation amplitude in time $\langle\tau\rangle = \langle\phi\rangle/\omega_s$ and substituting the analytic form into Eq. (4), we obtain

$$\langle\tau\rangle^2 = C^2 \left\{ \frac{8\eta\Delta t_1}{\pi\omega_s e V_{bb} \beta_s^2 E_s} \left[\frac{\sqrt{\frac{2}{\Delta t_1} \{\tau\} - (\Delta t_1 + \Delta t_2)}}{\sin^{-1} \left[\frac{\Delta t_1}{\sqrt{\Delta t_1^2 + 2\Delta t_1 \{\tau\} - (\Delta t_1 + \Delta t_2)}} \right]} + \frac{\Delta t_2}{\sqrt{\Delta t_1^2 + 2\Delta t_1 \{\tau\} - (\Delta t_1 + \Delta t_2)}} \right] \right\} \quad (5)$$

Eq. (5) is a transcendental function of $\langle\tau\rangle$. Note that the equation includes information about the initial condition of an individual particle through the term of C , the barrier conditions of V_0 , Δt_1 , and Δt_2 , and the parameters of ω_s , β_s , E_s , and η uniquely determined for a fixed accelerator. By solving Eq. (5), we can obtain the temporal evolution of the oscillation amplitude in time associated with the acceleration.

If the barrier condition is maintained to be a constant, a particle, the oscillation amplitude of which has initially extended to the flat barrier region (I), will fall in the linear barrier region (II) as a result of the adiabatic damping. In this situation, Eq. (5) becomes invalid. The instantaneous oscillation amplitude in time must satisfy the following relationship,

$$\langle\tau\rangle^2 = C^2 \left\{ \frac{8\eta\Delta t_1}{\pi\omega_s e V_{bb} \beta_s^2 E_s} \left[\frac{\pi}{2} + \frac{\Delta t_2}{[\langle\tau\rangle - \Delta t_2]} \right] \right\}, \quad (6)$$

where C is determined from the boundary condition. Consequently, Eq. (5) and Eq. (6) gives the oscillation amplitude in the regions where $\langle \tau \rangle > (\Delta t_1 + \Delta t_2)$ and $\langle \tau \rangle < (\Delta t_1 + \Delta t_2)$, respectively. These two solutions should be connected at $\langle \tau \rangle = (\Delta t_1 + \Delta t_2)$.

The present result has been obtained assuming the trapezoidal profile of the barrier voltage. It is straightforward to know the temporal evolution of the oscillation amplitude $\langle \tau \rangle$ for more extreme profiles, such as a rectangular profile ($\Delta t_1=0$), a short profile ($\Delta t_2=0$), and a discrete profile ($\Delta t_1=\Delta t_2=0$). For the rectangular profile,

$$\langle \tau \rangle^2 = C^2 \sqrt{\frac{8\eta}{\pi\omega_s e V_{bb} \beta_s^2 E_s}} \left\{ \sqrt{2(\langle \tau \rangle - \Delta t_2)} + \frac{\Delta t_2}{\sqrt{2(\langle \tau \rangle - \Delta t_2)}} \right\} \quad (7)$$

This form mostly suggests a particular feature of the adiabatic damping in the induction synchrotron, which can be distinguished from that in RF synchrotrons. A solution of Eq. (7) is always written in terms of $\langle \tau \rangle = g(t, \Delta t_2) + \Delta t_2$, where $g(t, \Delta t_2)$ is a slowly varying function of t and is subjected to adiabatic damping and gradually becomes smaller. Since the isolated offset term of Δt_2 is controllable, the oscillation amplitude can be maintained in a well controlled manner throughout the acceleration, as expected.

COMPARISON WITH SIMULATION AND EXPERIMENTAL RESULTS

Experimental results and analytical predictions can be compared only after loss at the beginning of acceleration, i.e. from 0.633 sec from injection. From this time onwards bunch shrinking can be attributed only to adiabatic damping. Assuming an initial bunch length of 190 nsec, which was taken from the experimental result at $t=0.633$ sec, the theoretical prediction is plotted in Fig. 3. Ideal simulation result for a trapezoidal barrier is plotted in Fig.4. where Eq.(5) and Eq.(6) were used for the case when $\langle \tau \rangle > (\Delta t_1 + \Delta t_2)$ and $\langle \tau \rangle < (\Delta t_1 + \Delta t_2)$, respectively. We can see that both are in fairly good agreement.

SUMMARY

A novel theory to estimate adiabatic damping phenomenon in the induction synchrotron has been presented. The theory is based on an analogy of the WKB solution for a harmonic oscillator, the parameters of which slowly vary in time. It has turned out that the theory can quantitatively explain the experimental results. In RF synchrotrons the bunch size infinitely shrinks beyond transition energy. We know that this is intrinsic feature in the RF synchrotrons. However, this is not the case in an induction synchrotron. The bunch-length in an induction synchrotron is mainly determined with the time duration between barrier voltages as expected. This fact has been proven mathematically. There is an another approach also to give the temporal evolution of the longitudinal beam envelope, which is determined by the

equation, $d^2\rho/dt^2 + Q^2(t)\rho = 1/\rho^3$. Assuming that everything is in a steady-state and the oscillation system is linear, then the envelope solution is straightforwardly written by $\rho = [1/Q(t)]^{1/2}$, where the frequency of the linear system $Q(t)$ is a priori assumed to be a frequency of the synchrotron motion averaged in a single turn. Unfortunately this logic is not justified, because the envelope equation is an auxiliary equation to the time-dependent linear equation and both is always a pair. Though the present approach is based on the hypothesis, it will create a stir in the adiabaticity problem in nonlinear periodic motions.

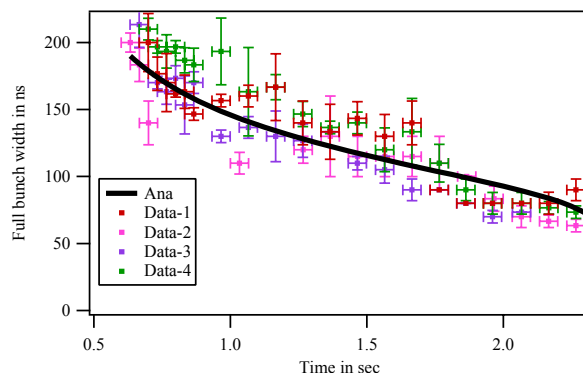


Figure 3: Comparison between the experimental results and theoretical predictions after 0.633 sec from injection.

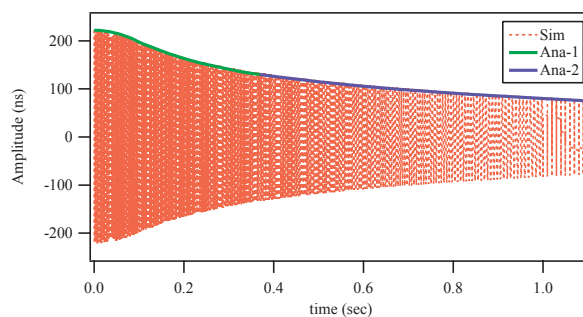


Figure 4: Comparison between the simulation results and theoretical predictions for ideal trapezoidal barrier.

REFERENCES

- [1] K.Takayama and J.Kishiro, *Nucl. Inst. Meth. in Phys. Res. A* 451, (2000) p. 304-317.
- [2] K.Takayama *et al.*, *Phys. Rev. Lett.* 94, (2005) p. 144801-4.
- [3] K.Torikai *et al.*, KEK Preprint 2005-80 (2005), submitted for publication.
- [4] K.Takayama *et al.*, "Experimental Demonstration of the Induction Synchrotron", *Phys. Rev. Lett.* 98 (2007).
- [5] K.Takayama *et al.*, "Experimental Demonstration of the Induction Synchrotron", in this proceedings, TUXC02.
- [6] T.Dixit, Y.Shimosaki, and K.Takayama, submitted for publication (2007).